An Automatic Equipment for the Marking of 12" Polyethylene Pipes

Jefferson Corbera, Fabricio Guillén, Mario De La Cruz, Guillermo Kemper, José Oliden
School of Electronic Engineering
Universidad Peruana de Ciencias Aplicadas (UPC)
Lima 15023, Perú

ABSTRACT

This work proposes a device for automatically marking high-density polyethylene (HDPE) tubes, using a mechatronic system which moves through the outside of the tubes and marks symmetrical points along it, to be used as perforation guides. Due to their physical and chemical properties, these tubes are widely used in draining processes in the mining and petrochemical industries, and the proposed system is an integral solution for the tube manufacturing industry. Current commercial solutions use costly methods which employ large anchored machinery for marking and perforation. Other available products use laser marking systems. The present work proposes a portable, low-cost, and easy to use system with a friendly user interface. It employs an integrated system which uses electronic control of geared motors and encoders to control the linear displacement along 12 inch HDPE tubes. Said displacement is done by a lightweight structure equipped with electrical pistons anchored to a mechanical system. A graphic user interface aids in configuring the marking process. The process ends when the whole tube has been marked and is ready for the subsequent drilling process. Validation testing shows that the system achieves a marking location precision of 95%. Thus, the present work successfully achieves its purpose.

Keywords: magnetic encoder, HDPE, electrical piston, tube marking, automatic marking, draining tube, mining.

1. INTRODUCTION

In recent years, high-density polyethylene (HDPE) has achieved popularity in an array of industries. HDPE presents a year-over-year growth of 2.7% in the Asia-Pacific region [1], mainly in the dairy, fluid transport and mining industries. In the latter case, HDPE has been mainly used in draining tubing systems to filter mining residues and waste. These waste byproducts have to be carefully handled to avoid environmental damage.

This application requires tubes to be precisely drilled in linear and radial patterns to avoid unwanted waste spills. Thus, the tube preparation process has 2 stages: hole marking and hole drilling.

The proposed equipment automatically performs the marking process with minimal hole positioning error.

Commercial solutions that also address this problem are described:

In [2], a carbon dioxide (CO_2) laser performs the marking. This solution has the flexibility of marking diverse shapes like circles, triangles, and squares. Nonetheless, there is a perpendicular deviation of 5 mm. Also, the process generates scoring which negatively impacts the tube surface rugosity. Finally, maintenance costs are high due to the components and gas for the laser.

The solution presented in [3] proposes computer numerical control (CNC) machines to mark large tubes. The process is very effective but requires many steps prior to the marking itself. Besides, tube centering and positioning are time consuming and labor intensive. Finally, CNC machines are large and non-portable.

Scientific literature also presents proposals to solve the marking issue. The authors in [4] present a device to automatically inspect the inside of 6” to 8” tubes. [5] and [6] propose a solution to inspect the outside of tubes with robots adhered to the tube surface. This is done to detect gas or oil leaks.

These proposed solutions are not appropriate for the marking process, due to their slow locomotive process caused by the processing time required to execute the leak detection.

Finally, manual marking is also an available solution, which requires many operators to be located along the tube. Marking is done with the aid of a measuring tape. First, linear marking is done and then the tube is rotated to a reference point. This point allows the operators to repeat the linear marking until all the holes are marked. The main disadvantages of this process are its high labor intensity and the dependance of marking precision on the ability of the operators. This ability can be hampered by tiredness and sensory limitations.

This work presents a novel automatic marking equipment which successfully fulfills effectiveness, portability, and ease of use requirements. The system uses encoder-equipped geared motors to achieve linear displacement and electrical pistons anchored to the mechanical structure.

Marking occurs along a linear path over a 12 meter long tube with a 12” diameter.

At the end of the displacement, markings will be linearly and radially distributed over the tube to signal the drilling positions.

Finally, validation shows that the developed systems achieves a 95% precision regarding the desired marking positions.

The following sections describe the stages of the proposed system.

2. PROPOSED EQUIPMENT DESCRIPTION

Fig. 1 shows the proposed equipment block diagram. The marking process starts by inputting configuration data, and positioning and installing the device over the HDPE tube (Fig. 2).

Next, the operator orders the Controller to start the Marking control process and the structure Movement control process.

The process requires adequate motor control precision and sound mechanical structure design. This will allow the marking points to be in the correct positions with minimal error and within established tolerances.

The following sections describe the system parts, their functions, and their interactions.

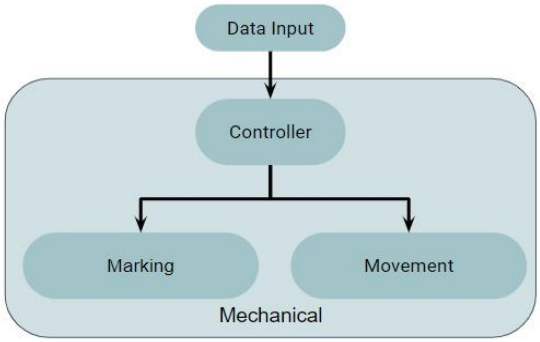

Fig. 1. Equipment block diagram

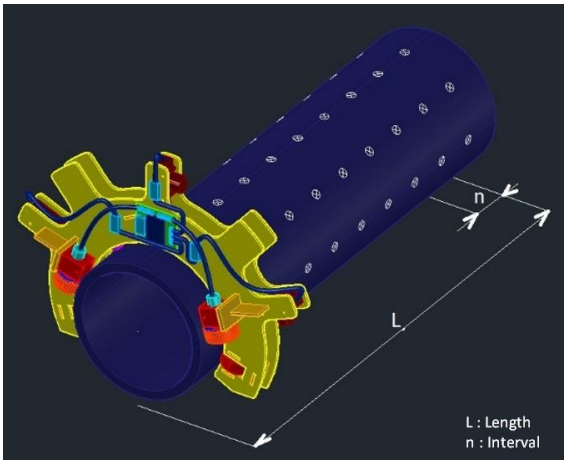

Fig. 2. Equipment developed for the marking process

2.1. Data input

The equipment receives configuration and operation data from a custom mobile app. The user inputs the tube length and the distance between markings.

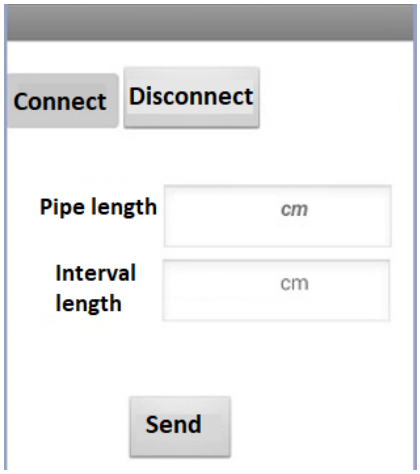

Fig. 3. Layout of the application.

Fig. 3 shows the app's user interface. The app allows the input of the following parameters:

a. Connect/disconnect buttons
These buttons link the app to the device via a Bluetooth module, which indicates the establishment of a link so data can be sent.

b. Text box: pipe length
Serves to input the tube/pipe length, which is sent to the microcontroller.

c. Text box: Interval length
Serves to input the distance between marking points, in centimeters. This datum is sent to the microcontroller.

d. Send button
This button sends the data to the microcontroller for later computations.

2.2. Movement

Motor spin determines the equipment's movement. The motor must spin a certain angle to move the structure the desired distance along the tube. This angle is calculated with the radius of the equipment's wheel.
Fig. 4. shows a representation of the wheel over the tube.

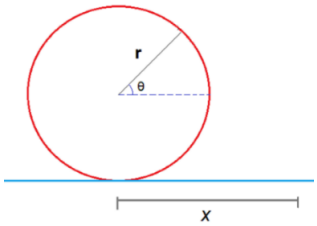

Fig. 4. Representation of the wheel

The user inputs the displacement distance via the app. The wheel radius is known to be $r = 3.5$ cm.
These values serve to calculate the motor's desired spin angle, using the following equation [7]:

$$X = r \times \theta \tag{1}$$

Where θ is the spin angle and X is the desired length.

2.3. Controller

The displacement and marking controller is described in 3 steps: system identification, PID (proportional-integral-derivative) controller design and hardware implementation.

a. System identification

Controller design requires finding the system's transfer function, which was done with the reaction curve method [8], described below.

Step 1: find the motor's transfer function
First, the motor speed after power up is obtained. The curve is shown in Fig. 5.

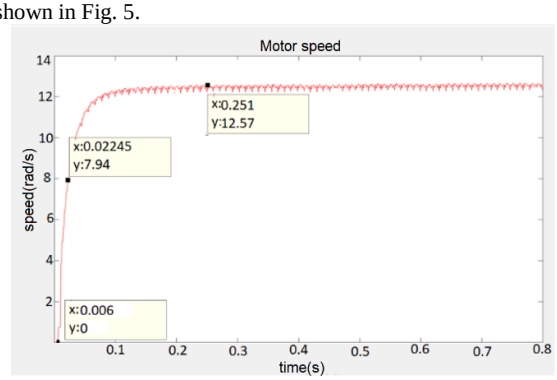

Fig. 5. Speed graph to find K of the left engine.

The curve shows a delay after power up. This implies that the motor step response can be modelled by the following transfer function:
.

$$G(s) = \frac{K}{\alpha s + 1} e^{-\tau s} \tag{2}$$

Where K is the system gain, α the time constant and τ the delay.

Step 2: find the motor speed transfer function's parameters values

Fig. 5 shows the stable speed value (V_{final}), which was considered as $K = V_{final} = 12.57$ rad/s.
To find α and τ, firstly the point where speed reaches 63.2% of the stable amplitude must be found. This was done with the following equation:

$$V1 = 0.632 \times V_{final} = 0.632 \times 12.57 = 0.794 \text{ rad/s} \quad (3)$$

Fig. 5 shows that the motor reaches speed $V1$ at 0.022 seconds, which will be the value of α[8].
Then, the delay was defined as the time it took for the curve in Fig. 5 to differ from zero. Thus, the delay was of $\tau = 0.006$ seconds.
Finally, the motor speed transfer function is:

$$G(s) = \frac{12.57}{0.022s + 1} e^{-0.006s} \quad (4)$$

Step 3: find the motor angular position continuous transfer function's parameters values

The motor speed transfer function has to be integrated to find the motor position transfer function, which will be controlled. This results in the following motor angular position transfer function:

$$G_p(s) = \frac{G(s)}{s} = \frac{12.57}{s(0.022s + 1)} e^{-0.006s} \quad (5)$$

Fig. 6 shows the system block diagram. Fig.7 shows the angular position as the output of $G_p(s)$.

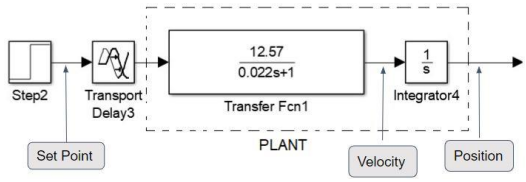

Fig. 6. Angular position block diagram

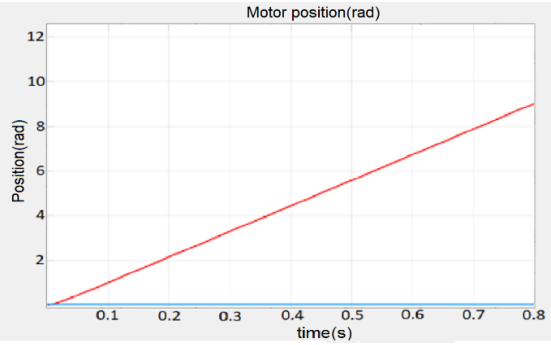

Fig. 7. Response to a step of the angular position without controller.

Step 4: discretize the motor angular position continuous transfer function.

The continuous transfer function $G_p(s)$ was discretized with a sampling time of 1 ms, which is appropriate and coherent with regards to the microcontroller used in this work (ESP32).

The bilinear transform [9] was applied to $G_p(s)$ to obtain the following discrete time transfer function:

$$G_p(z) = z^{-6} \times \frac{0.0002814 \times z + 0.0002772}{z^2 - 1.956 \times z + 0.9556} \quad (6)$$

b. PID controller design

PID systems are widely used in diverse industrial applications. These are useful when controlling systems for which the transfer function is unknown and when needing an adequate precision of the control system [9].

The transfer function of a discrete PID controller is:

$$C(z) = Kp + \frac{Ki}{1 - z^{-1}} + Kd \times (1 - z^{-1}) \quad (7)$$

Where:

Kp: Proportional gain coefficient

Ki: Integral gain coefficient

Kd: Derivative gain coefficient

A heuristic approach was used to tune the controller parameters. The Kp, Ki and Kd parameters were configured to then collect the movement data. These parameters were gradually and consecutively adjusted until the desired output precision was achieved.
Only the proportional parameter was configured for the first test: $Kp = 10$, $Ki = 0$, $Kp = 0$. Fig. 8 shows the obtained response for a 10 cm set point.
The controller achieves a value close to the set point, with a slight stationary error.

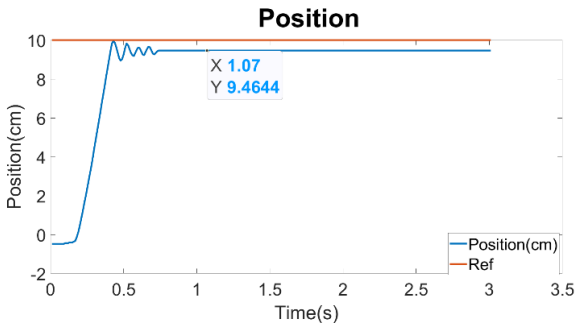

Fig. 8. Response to a 10(cm) step with $Kp = 10$ controller, $Ki = 0$, $Kd = 0$.

When the reference was reduced to 4 cm (Fig. 9), it became evident that the proportional controller by itself could not reach the set point, since the response falls short of achieving the desired motor rotation.

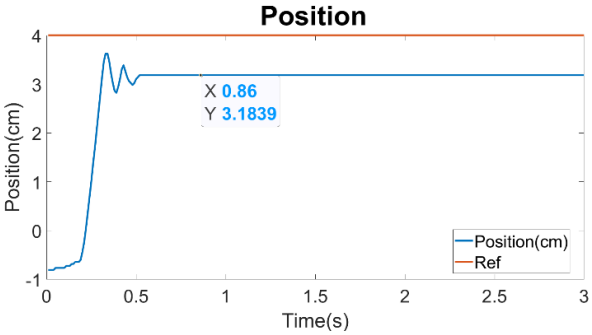

Fig. 9. Response to a 4cm step with $Kp = 10$ controller, $Ki = 0$, $Kd = 0$.

This was solved by increasing the proportional constant value and configuring the integrator: $Kp = 50$, $Ki = 0.05$ and $Kd = 0$. Fig. 10 shows the resulting response.

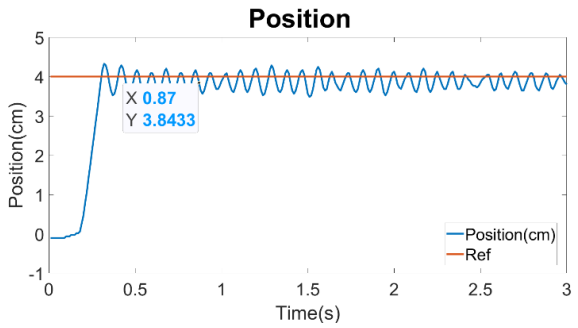

Fig. 10. Response to a 4cm step with $K\mathrm{p} = 50$ controller, $K\mathrm{i} = 0.05$, $K\mathrm{d} = 0$.

Fig. 10 shows a strong oscillation which would impede the correct control of the system due to instability. Thus, the derivative control was configured to reduce said instability and stabilize the signal.

After many tests, the configuration which achieved the best results was: $K\mathrm{p} = 50$, $K\mathrm{i} = 0.05$, $K\mathrm{d} = 20$. Fig. 11 shows the obtained response.

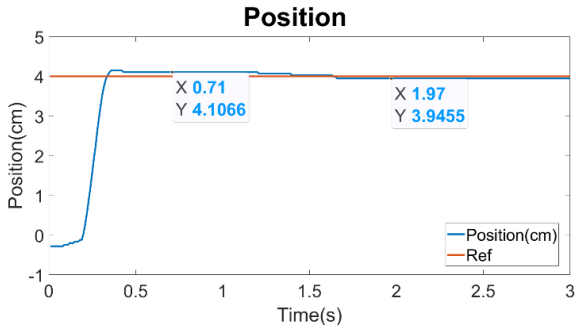

Fig. 11. Response to a 4cm step with $K\mathrm{p} = 50$ controller, $K\mathrm{i} = 0.05$, $K\mathrm{d} = 20$.

After designing the PID controller, it was implemented on the equipment and thoroughly tested, to verify an adequate performance. The successful results of this validation are shown in Fig. 12.

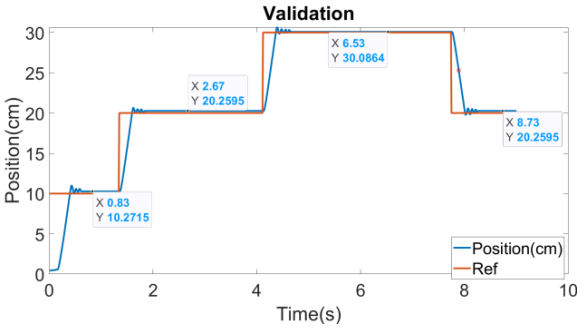

Fig. 12. Controller validation

2.4. Marking

Tube marking requires the motors and wheels to reach the desired position. Once in the stable position, a signal activates the pistons which move a seal and mark the point in the tube.
The piston movement control was done via the H-bridge in the L298N module, as shown in Fig. 13.
This module also permitted the control of the motor movement, where each motor drew 2 A with a 12 V power supply [10].

2.5. Mechanical structure

The mechanical structure was designed to stabilize and bear the actuator load during the marking process. The structure consists of two truncated rings. Fig. 13 shows that the structure's base holds the wheels which enable the linear displacement over the tube surface. Moreover, the pistons are mounted on the structure, such that the center of mass is located close to the tube center. This favors structural rigidity during the marking process (Fig. 14).

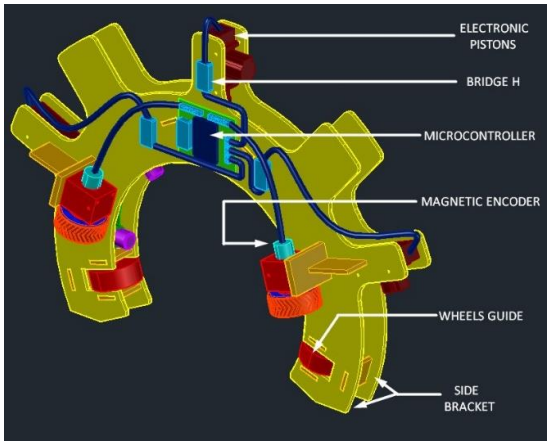

Fig. 13. Developed equipment and electrical parts.

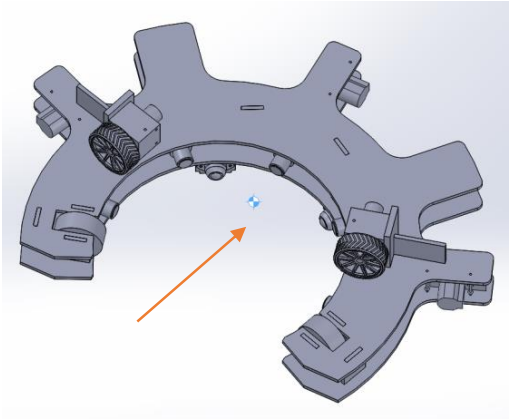

Fig. 14. Components distribution and center of mass location of the mechanical structure.

Fig. 15 shows the block diagram of the electronic circuit. It is composed by an ESP32 controller which receives the tube size data via a bluetooth module. Next, the information is processed and activation signals are sent to the wheel motors. The microcontroller permanently knows the motor position through the use of encoders.

The microcontroller will send a signal to the H-bridge such that the motor spins in the correct direction in case the motor under- or overshoots the desired position.
Once the equipment stabilizes in the desired position, the microcontroller stops the motors and sends a signal to the piston H-bridge. The electrical pistons expand to perform the marking, compress and repeat the process until all the markings are performed.
The microcontroller calculates the total number of markings by dividing the tube length by the marking interval (Fig. 2).

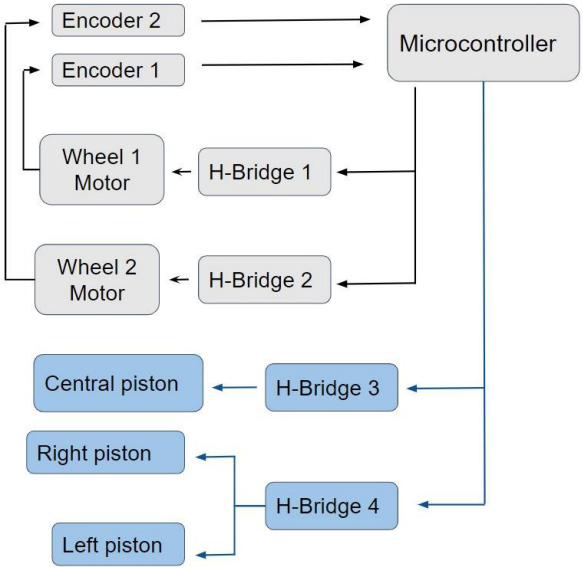

Fig.15. Electronic block diagram.

3. RESULTS

Testing was done in a 2 meter long tube with a diameter of 12 inches. Data was sent through the mobile app and the equipment's correct performance was verified. The chosen performance metric was the absolute error, expressed in equation 8:

$$E_a = V_{deseado} - V_{obtenido} \tag{8}$$

Where $V_{deseado}$ is the desired value and $V_{obtenido}$ is the value obtained by the equipment.

The relative error E_r was also used:

$$E_r = \frac{V_{deseado} - V_{obtenido}}{V_{deseado}} \times 100\% \tag{9}$$

Both errors help in evaluating the equipment's correct performance.
The acceptable error was defined as ±0.5 cm [11]. This value was used to validate that the drill markings are symmetrical along the tube.
The relative error helped as a quality metric of the equipment. Larger marking distances resulted in a lower relative error and thus a better quality. Nonetheless, the best metric was the absolute error, due to uncertainty issues.

Table 1 shows the results for each reference.
The developed system has a successful performance, since the error values are below the acceptable errors specified by users.

4. CONCLUSIONS

Controller design was done by a heuristic approach, with precise results. The decision of using this method was taken because of the complexity of obtaining a precise system model, due to frictional forces between the wheels and the tube surface. Also, it is challenging to find the exact position where the motors should be located, in order to efficiently move the equipment over the tube.

Table 1. Results to different reference points.

N°	Set-Point (cm)	Obtained position (cm)	Relative Error (%)	Absolute Error (cm)
1	3	3.1	-0.033	-0.1
2	3	3.1	-0.033	-0.1
3	3	3.4	-0.133	-0.4
4	3	3.35	-0.117	-0.35
5	3	3.5	-0.167	-0.5
6	3	3.4	-0.133	-0.4
7	3	3.3	-0.100	-0.3
8	3	3.4	-0.133	-0.4
9	3	3.4	-0.133	-0.4
10	3	3.4	-0.133	-0.4
11	10	9.7	0.030	0.3
12	10	9.9	0.010	0.1
13	10	10.2	-0.020	-0.2
14	10	10.3	-0.030	-0.3
15	10	10.1	-0.010	-0.1
16	10	10.05	-0.005	-0.05
17	10	10.21	-0.021	-0.21
18	10	10.3	-0.030	-0.3
19	10	10.2	-0.020	-0.2
20	10	10.2	-0.020	-0.2
21	20	20.2	-0.010	-0.2
22	20	20.1	-0.005	-0.1
23	20	20.1	-0.005	-0.1
24	20	19.7	0.015	0.3
25	20	19.7	0.015	0.3
26	20	19.8	0.010	0.2
27	20	19.8	0.010	0.2
28	20	19.6	0.020	0.4
29	20	19.8	0.010	0.2
30	20	19.5	0.025	0.6
31	30	29.7	0.010	0.3
32	30	29.7	0.010	0.3
33	30	29.7	0.010	0.3
34	30	30.1	-0.003	-0.1
35	30	30.2	-0.007	-0.2
36	30	30.2	-0.007	-0.6
37	30	30.2	-0.007	-0.2
38	30	29.7	0.010	0.3
39	30	29.7	0.010	0.3
40	30	30.0	0.010	0.3

5. REFERENCES

[1] Interempresas. 2017. El Polietileno De Alta Densidad Crecerá Un 2,7% Anual Hasta 2024. [Internet] Available at: <https://www.interempresas.net/Plastico/Articulos/194951-Situacion-internacional-del-polietileno-HDPE.html>

[2] Al-Qaisy, S. J. S. y Karatas, C. **"Láser Cutting of High Density Poly Ethylene (Hdpe) Pipes Pe100 using Co2 Gas Laser",** Revista Internacional de Ingenieria y Tecnología Avanzada (IJEAT). ISNN: 2249-8958, Volume-9 Issue-1,octubre de 2019.

[3] Salvatierra, José Refugio Villaseñor, Ramón Chávez Bracamontes, and Humberto Bracamontes del Toro. "**Desarrollo de prototipo estandarizado en código abierto para marca y corte de materiales mediante tecnología láser** (Development of standarized open source prototype for brand and cutting of materials using laser technology)." Pistas Educativas 41.134 (2019).

[4] Castillo-Castañeda, E. y Córdoba-Malaver, R. "Mobile Robot with Wheeled-Legs for Inspection of Pipes with Variable Diameter and Elbow Shapes", **Mechanisms and Machine Science**, Volume-93, pp. 325-331, 2021.

[5] Amarasinghe, R., Baokun, H., Jayasundara, C. y Mudugamuwa, A. "Development of a robotic system with stand-alone monocular vision system for eco-friendly defect detection in oil transportation", **Smart Innovation, Systems and Technologies**, Volume-200, pp. 107-118, 2021.

[6] Budianto, A., Muhtadan, Dipta, IMY. and Iman, AN. "Development of Liquefied Petroleum Gas (LPG) leakage detection wheeled robot on horizontal pipes based on Arduino Uno", **Journal of Physycs: Serie de conferencias**, Volume 1511, junio de 2020.

[7] Jimenez, L. **"Longitud de Arco y Sector Circular"**, Proyectable, México. 2017 [Internet] Available at: <http://hdl.handle.net/20.500.11799/79721>

[8] Vergara-Betancourt, A., Salazar-Hidalgo, E. and Zapata-Nava, O. "Obtención de la función de transferencia de un motor de DC mediante el análisis de la curva de reacción." **Revista de Aplicación Científica y Técnica** (2017).

[9] K. Ogata, **"Ingeniería de Control Moderno"**, Pearson Eduación S.A., Madrid, España, vol. 5, N° 12, pp. 582-589,2010.

[10] Instructables (2014, Nov. 25). "Driver l298n". [Internet]. Disponible en Control-DC-and-stepper-motors-with-L298N-Dual Moto/.

[11] Orozco, M**., "Sistemas de subdrenaje en obras de estabilizacion",** proyecto de grados, escuela colombiana de ingenieria julio garavito especializacion en recursos hidraulicos y medio ambiente bogota, bogota, colombia, 2007.